Catalysis Letters
https://doi.org/10.1007/s10562-019-03088-9

Hydrazinylbenzenesulfonic Acid-Modified Nieuwland Catalyst for Acetylene Dimerization Reaction

Qixia Zhang[1] · **Congcong Li**[1] · **Juan Luo**[1] · **Jianwei Xie**[1] · **Jinli Zhang**[2] · **Bin Dai**[1]

Received: 15 October 2019 / Accepted: 21 December 2019

Abstract

A novel Nieuwland catalytic system, containing 5 mol% of 4-hydrazinylbenzenesulfonic acid (**S_8**), was developed and exhibited an excellent catalytic performance and good stability in the acetylene dimerization reaction. The acetylene conversion reached 57.1%, while the selectivity of monovinylacetylene (MVA) was 75.1%. The yield of MVA was maintained at 42.9% under an acetylene gas hourly space velocity (GHSV) of 80 h^{-1} at 80 °C, which was increased by 18.8% over the control Nieuwland catalytic system. The addition of **S_8** increased the dissolution of CuCl in water, inhibited the polymer formation, and hindered the Cu^+ loss during the reaction process, thus improving the activity and the long-term stability of the modified Nieuwland catalyst.

Graphic Abstract

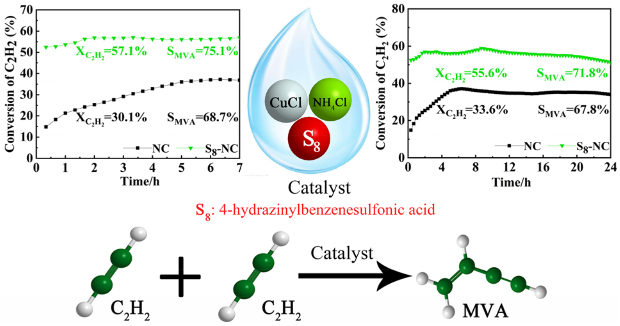

Keywords Acetylene dimerization · Monovinylacetylene · Modified Nieuwland catalyst · Cu-based catalyst

1 Introduction

Chloroprene rubber (CR) is a synthetic polymer rubber material with broad application prospects in various fields of production and life. Catalytic dimerization of acetylene over the Nieuwland catalysts (NC), which is performed with the dissolution of CuCl, NH_4Cl (or KCl) and HCl in water to produce monovinylacetylene (MVA) [1, 2], is an important industrial process of the acetylene-based CR production [3–5]. Despite years of efforts in the development and improvement of the NC, obstacles still exist, such as the low acetylene conversion and the poor MVA yield.

Recently, second-metal-added [6–9] or catalyst-ligand modification methods [10–13] that enhance the catalytic

---

Electronic supplementary material The online version of this article (https://doi.org/10.1007/s10562-019-03088-9) contains supplementary material, which is available to authorized users.

✉ Jianwei Xie
cesxjw@foxmail.com

[1] School of Chemistry and Chemical Engineering/Key Laboratory for Green Processing of Chemical Engineering of Xinjiang Bingtuan, Shihezi University, North 4th Road, Shihezi 832003, China

[2] School of Chemical Engineering and Technology, Tianjin University, Tianjin 300072, China

efficiency and selectivity of the acetylene dimerization have been suggested. For example, Liu et al. have reported the addition of $LaCl_3$ in NC can inhibit the formation of divinylacetylene (DVA) and polymer, and improve selectivity of MVA. The ratio of MVA/DVA in the gas phase product increased from 6 to 19, and the selectivity of MVA increased from 80 to 95% at 80 °C [7]. Chen et al. have reported the effect of substituted acetic acid as a catalyst promoter of the acetylene dimerization reaction in NC. The addition of thioglycolic acid ligands in NC changed the mechanism of acetylene dimerization and the selectivity of acetaldehyde reached 99.7% [10]. In 2016, Liu found that the addition of Cu^{2+} in anhydrous NC inhibited the oxidation of Cu^+ into Cu^{2+} and enhanced the catalytic performance and lifetime. It can achieve 40% conversion of acetylene with a molar ratio of Cu^+ to Cu^{2+} of 2:1 [6]. Recently, it was proven that the addition of nitrogen-containing carboxylic acids [11, 12] increases the conversion of acetylene, the selectivity of MVA and the catalyst lifetime because of their ability to strongly coordinate and stabilize the Cu^+ ions. The yield of MVA in NC containing *N*-(2-acetamido) iminodiacetic acid was 17.1% higher than that of NC [12].

Sulfonic acids, a class of organic compounds containing the $–SO_2OH$ group, are employed as catalysts in various reactions, while they are used as additives for the modification of known catalytic systems [14–17]. Lately, Amoozadeh et al. have reported several sulfonic acid modified catalysts. Particularly, in 2015, they revealed nano-WO_3-supported sulfonic acid as an efficient and highly recyclable heterogeneous nano-catalyst for organic reactions [14]. Meanwhile, nano-γ-Fe_2O_3–SO_3H, a nanomagnetic-supported sulfonic acid, was developed for the Hantzsch condensation [15]. In 2016, nano-ZrO_2–SO_3H was disclosed with several advantages such as low cost, low toxicity, ease of preparation, good stability, high reusability, and operational simplicity [17]. They suggested that nano-MO_X–SO_3H (M = W, Fe or Zr) acts as a Lewis and a Brønsted acid simultaneously (sulfonic acids acts as the Brønsted acid and nano-MO_X acts as Lewis acid). Hydrogen bonds provided by Brønsted acid initiates the catalytic process. Compared with nano-MO_X, nano-MO_X–SO_3H has better catalytic activity, good stability and high reusability. In the study of acetylene dimerization, Deng et al. found that the catalyst activity was improved by adding hydrochloric acid to control the pH [18]. We previously found that the addition of nitrogen-containing carboxylic acids increases the MVA yield and the catalyst lifetime because of strong coordination between ligands and Cu^+ [12]. These interesting results inspired us to study whether the sulfonic acids can improve NC during acetylene dimerization.

This study describes the development of a novel modified Nieuwland catalyst using sulfonic acids and its application on the acetylene dimerization reaction. A series of distinct sulfonic acid derivatives were applied, and their efficacy was evaluated based on the resulting acetylene conversion and the MVA selectivity. Moreover, the effects of the sulfonic acids on the catalyst structure and its active components were examined through various techniques, including transmission electron microscopy (TEM), X-ray diffraction (XRD), Fourier-transform infrared spectroscopy (FT-IR), thermogravimetry/derivative thermogravimetry (TG/DTG), temperature programed desorption-mass spectrometry (TPD-MS), inductively coupled plasma spectroscopy (ICP), and X-ray photoelectron spectroscopy (XPS).

2 Experimental

2.1 Materials

4-Aminobenzenesulfonic acid (**S_1**), 2-(bis(2-hydroxyethyl)amino)ethane-1-sulfonic acid (**S_2**), 2-((1,3-dihydroxy-2-(hydroxymethyl)propan-2-yl)amino)ethane-1-sulfonic acid (**S_3**), 2,2′-(piperazine-1,4-diyl) bis(ethane-1-sulfonic acid) (**S_4**), sulfamic acid (**S_5**), 5-aminonaphthalene-1-sulfonic acid (**S_6**), benzenesulfonic acid (**S_7**), 4-hydrazinylbenzenesulfonic acid (**S_8**), CuCl (99%), and NH_4Cl (purity ≥ 99.5%), were purchased from Adamas-beta and directly used without purification.

The catalyst used as control was labeled as NC and the catalysts containing **S_x** additive were denoted as **S_x**-NC, where x is the ligand number. The amount of each **S_x** was calculated in mole, based on the CuCl. The structures of the eight sulfuric acid ligands are shown in Table 1.

2.2 Catalyst Preparation

The NC was prepared by dissolving 5.35 g (0.1 mol) of NH_4Cl and 9.9 g (0.1 mol) of CuCl in 10 ml of deionized water at 80 °C, a reddish-brown homogeneous mixture was obtained. Then, a certain mole amount of **S_x** was added to the NC, which varied among the eight applied ligands, based on the CuCl quantity.

Before the reaction, the reactor was purged with nitrogen to eliminate the air. Then, 5.35 g of NH_4Cl and 10 mL of deionized water were added at 80 °C. After 10 min of stirring, 9.9 g of CuCl and a certain amount of each ligand, which varied among the distinct sulfonic acids, were added in the above solution under nitrogen atmosphere. Stirring continued for at least 15 min, until the solids had completely dissolved, and the modified catalyst was obtained.

The fresh NC and **S_x**-NC, and the used NC and **S_8**-NC were left in the refrigerator at 3 °C for 6 h (NC and **S_8**-NC after 7 h of reaction was defined as used NC and **S_8**-NC). Then they were filtered from the catalytic solution, washed

Table 1 Additive and catalytic performance of **S_1**-NC–**S_8**-NC in acetylene dimerization

Additive		Acetylene conversion (MVA selectivity)[a]				
Name (number)	Structure	0.6 h	1.6 h	3 h	4.6 h	6 h
None	None	25.0% (69.6%)	31.3% (68.9)	33.7% (68.2%)	32.2% (67.5%)	31.8% (68.7%)
4-Aminobenzenesulfonic acid (**S_1**)	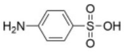	31.0% (72.2%)	34.0% (72.3%)	38.8% (72.8%)	40.8% (72.2%)	41.2% (71.5%)
2-(bis(2-hydroxyethyl)amino)ethane-1-sulfonic acid (**S_2**)	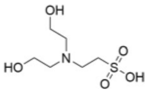	34.9% (68.1%)	39.2% (71.4%)	44.0% (72.1%)	43.6% (72.5%)	42.3% (72.1%)
2-((1,3-dihydroxy-2-(hydroxymethyl)propan-2-yl)amino)ethane-1-sulfonic acid (**S_3**)	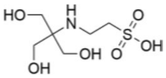	39.3% (75.4%)	39.5% (73.7%)	44.2% (74.0%)	45.9% (72.0%)	44.6% (71.8%)
2,2′-(piperazine-1,4-diyl) bis(ethane-1-sulfonic acid) (**S_4**)	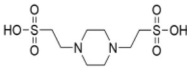	47.2% (72.2%)	46.1% (73.3%)	47.7% (74.6%)	45.0% (75.3%)	42.3% (75.0%)
sulfamic acid (**S_5**)	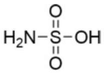	34.7% (69.0%)	34.4% (68.7%)	37.1% (70.1%)	39.0% (71.2%)	38.2% (71.4%)
5-Aminonaphthalene-1-sulfonic acid (**S_6**)	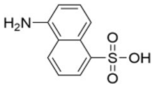	33.9% (78.8%)	34.0% (77.6%)	36.7% (76.6%)	37.1% (76.2%)	37.2% (76.4%)
Benzenesulfonic acid (**S_7**)	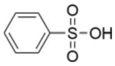	22.3% (70.1%)	24.7% (67.3%)	25.4% (64.1%)	25.1% (62.0%)	25.5% (61.4%)
4-Hydrazinylbenzenesulfonic acid (**S_8**)	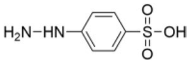	52.7% (71.5%)	50.4% (72.2%)	53.0% (73.6%)	54.9% (73.9%)	53.7% (73.4%)

Reaction conditions: Temperature (T) = 80 °C, GHSV(C_2H_2) = 105 h^{-1}, **S_x**:CuCl = 0.045:1

[a]Whole data was shown in Fig. S2

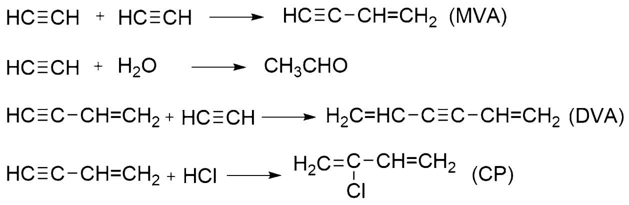

$$HC\equiv CH + HC\equiv CH \longrightarrow HC\equiv C-CH=CH_2 \text{ (MVA)}$$

$$HC\equiv CH + H_2O \longrightarrow CH_3CHO$$

$$HC\equiv C-CH=CH_2 + HC\equiv CH \longrightarrow H_2C=HC-C\equiv C-CH=CH_2 \text{ (DVA)}$$

$$HC\equiv C-CH=CH_2 + HCl \longrightarrow H_2C=\underset{Cl}{C}-CH=CH_2 \text{ (CP)}$$

Scheme 1 Gas phase products of the acetylene dimerization

with water and dried in a vacuum oven at 55 °C to obtain a solid catalyst, ready for characterization.

2.3 Acetylene Dimerization Reaction

The modified catalysts were tested in a self-designed bubble column reactor (length: 400 mm, outer diameter: 40 mm, inner diameter: 10 mm), which was used for the acetylene dimerization reaction (Fig. S1). Pure acetylene was then poured into the reactor. Immediately afterwards, the gas phase products (Scheme 1) were analyzed on-line by GC-2014C gas chromatograph (Shimadzu, GDX-301 and a flame ionization detector).

2.4 Determination of the Catalytic Performance

The criteria of the catalytic performance, namely the conversion of acetylene (X) and the selectivity of MVA (S) were defined by the following equations, respectively.

$$X = \frac{\lambda_2 + 2\lambda_3 + 2\lambda_4 + 3\lambda_5}{\lambda_1 + \lambda_2 + 2\lambda_3 + 2\lambda_4 + 3\lambda_5} \times 100\%$$

$$S = \frac{2\lambda_3}{\lambda_2 + 2\lambda_3 + 2\lambda_4 + 3\lambda_5} \times 100\%$$

where λ_1, λ_2, λ_3, λ_4, and λ_5 are the volume fractions of the gas products C_2H_2, CH_3CHO, MVA, CP, and DVA, respectively.

2.5 Methods for Catalyst Characterization

The pH of the catalyst was measured using a pen-like pH meter (Sanxin PHB-3). The FT-IR spectra of the samples were obtained using the Bruker Vertex70 FT-IR spectrometer (wavenumber range of 500–4000 cm^{-1}). TG/DTG experiments were performed using the NETZSCH STA 449 F3

Jupiter, under nitrogen atmosphere. The temperature ranged 50 °C–900 °C at an increasing rate of 10 °C/min. XRD patterns were collected using a Bruker D8 advanced X-ray diffractometer (10°–90° in 2θ). XPS data were recorded using a Kratos AXIS Ultra DLD spectrometer with a monochromatized Al-Kα X-ray source, the deconvolution of the XPS peaks are obtained by the XPSPEAK41 software to process XPS data. TEM images were recorded on a JEM2100F TEM instrument. The Micromeritic ASAP 2720 was used to obtain the TPD-MS experiments. The absolute content of Cu in all catalysts was determined using the ICP-AES technique (710ES, Varian, USA).

3 Results and Discussion

3.1 Catalytic Activity of NC and S_x-NC

Previously, we have reported that the addition of nitrogen-containing carboxylic acids [11, 12] can significantly enhance the catalytic performance of NC in acetylene dimerization. Inspired by these results, we initially tested the effect of four nitrogen-containing sulfonic acid additives, i.e., the 4-aminobenzene sulfonic acid (**S_1**), aliphatic chain nitrogen-containing sulfonic acids (**S_2** and **S_3**), and a nitrogen-containing heterocyclic sulfonic acid (**S_4**). The results of these experiments are presented in Table 1. All four additives exhibited higher acetylene conversion (> 40.0%) and MVA selectivity (> 70.0%) than the control NC, while the catalytic activity order was **S_4**-NC > **S_3**-NC > **S_2**-NC > **S_1**-NC > NC under the same reaction conditions.

We then screened the performance of alternative, including aryl substituted sulfonic acids (**S_5**–**S_8**) as additives for the investigated transformation (Table 1). Compared to other nitrogen-containing sulfonic acids, sulfamic acid (**S_5**) displayed relatively lower catalytic activity, revealing that the phenyl group is beneficial for the additive's efficiency. This was further confirmed by the replacement of the phenyl group with naphthalene (**S_6**), which led to a similar decreased catalytic activity. It is noteworthy that the additive without amino group (**S_7**) provided the worst activity among the present additives, suggesting that both the acidity of the sulfonic group and the coordination capacity of the amino group are essential for the catalytic activity. Replacement of the NH_2 group with the $NHNH_2$ moiety resulted in the **S_8**-modified NC (**S_8**-NC), which exhibited the highest average catalytic activity, with 53.0% of acetylene conversion, 72.9% of MVA selectivity, 38.63% of MVA yield, and satisfying stability. In addition, the reaction without an additive requires more than 2 h before reaching the highest acetylene conversion, but most of the additives forms the production highest performance within 1 h. In summary, **S_8** is the best additive among the examined, and resulted in high conversion and selectivity of MVA. Therefore, we next are focus on the effect of **S_8**-NC in the present transformation.

The loading of **S_8** was then investigated, and the results were shown in Fig. 1 (whole data in Fig. S3 and Table S1). Figure 1 shows relationship of C_2H_2 conversion after 0.6 h and 4 h to the amount of **S_8** additive. It suggests that increasing the additive increases the initial reaction rate, but the additive with higher content than 5% causes decrease of the C_2H_2 conversion. Too much additive may cause damage of the catalyst. Studies on reaction temperatures have shown that the most suitable temperature is 80 °C (Fig. S4 and Table S2). Investigation of the acetylene GHSV indicated the value of 80 h^{-1} as the most suitable rate (Fig. S5 and Table S3). Furthermore, the results of long-term stability experiments demonstrated that **S_8**-NC exhibited an excellent acetylene conversion, MVA selectivity, and stability over a 24-hour period (Fig. 2).

3.2 Catalyst Analysis

3.2.1 Effect of the S_8 Additive on the pH and Appearance of the Catalysts

Considering that the addition of the ligand **S_8** has a great influence on the reaction activity and that Cu^+ is the main catalytic component of the acetylene dimerization reaction, we characterized the fresh NC, **S_8**-NC and used NC **S_8**-NC catalysts investigating their structure and coordination ability.

Deng et al. stated that the pH value of the catalyst solution was adjusted to preserve a higher catalytic activity [18]. As shown in Table 2, **S_8**-NC possessed a lower initial pH

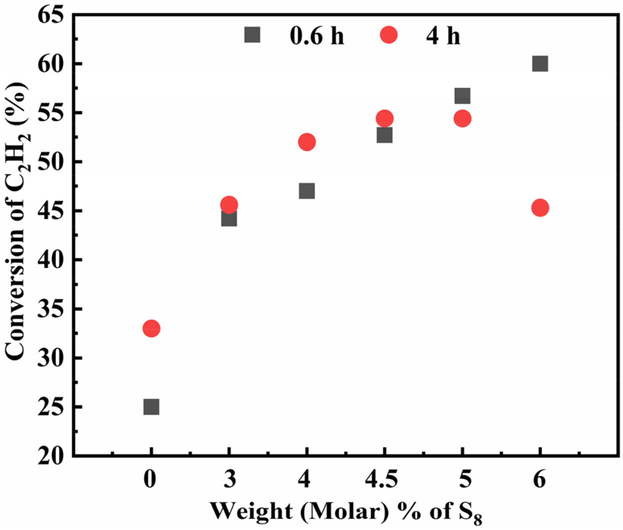

Fig. 1 Effect of the S_8 quantity on the acetylene dimerization. The whole data was shown in Fig. S3 and Table S1. Reaction conditions: T = 80 °C, GHSV(C_2H_2) = 105 h^{-1}

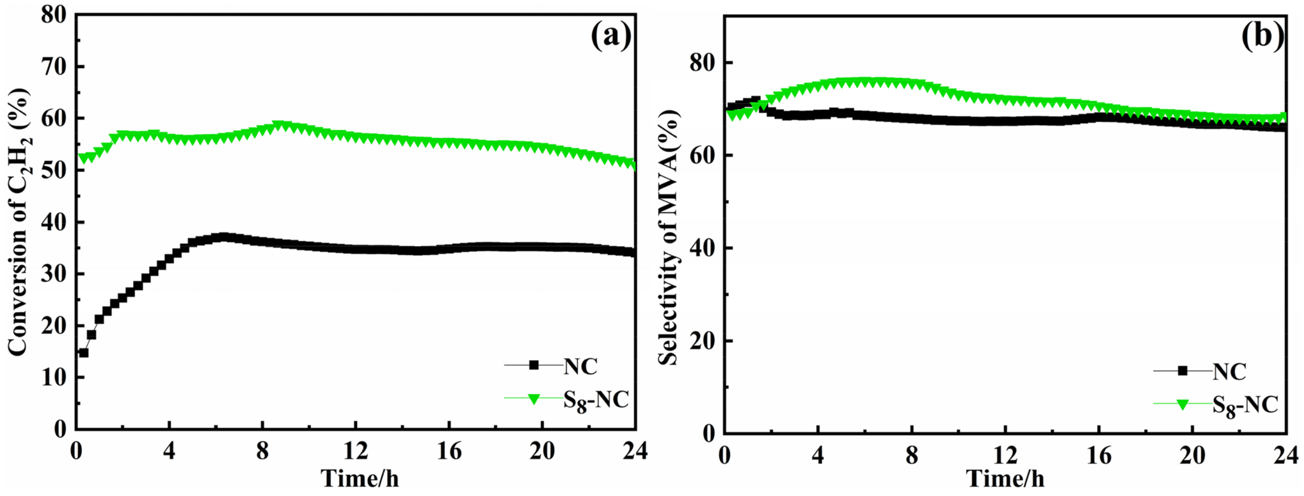

Fig. 2 Lifetime testing of NC and **S_8**-NC. **a** Acetylene conversion and **b** MVA selectivity in acetylene dimerization over **S_8**-NC. Reaction conditions: T = 80 °C, GHSV(C_2H_2) = 80 h^{-1}, **S_8**: CuCl = 0.05:1

Table 2 The pH of the NC and **S_8**-NC at different times during the acetylene dimerization reaction

Sample	pH							
	0 h	1 h	2 h	3 h	4 h	5 h	6 h	7 h
NC	1.1	1.1	1.2	1.1	1.2	1.3	1.3	1.3
S_8-NC	0.8	0.8	1.0	1.0	1.2	1.2	1.3	1.2

value, and over time the pH values of both catalytic systems remained almost similar. This because the **S_8** is an acidic amphoteric compound, which can reduce the initial pH value of **S_8**-NC solution. However, in the reaction solution, the acidic environment will inhibit the ionization of -SO_3H group and lead to both catalytic systems remained almost similar after the reaction time is longer than 2 h. The results indicated that the pH value is not a major activity index for the currently investigated catalyst.

Figure 3 depicts the reactor at different reaction times. It is clearly that the amount of precipitate was greater when NC was applied and consisted of the active Cu^+, C_2H_2, and NH_3 species [19]. In contrast, no obvious precipitate was observed using **S_8**-NC, explaining the higher catalytic

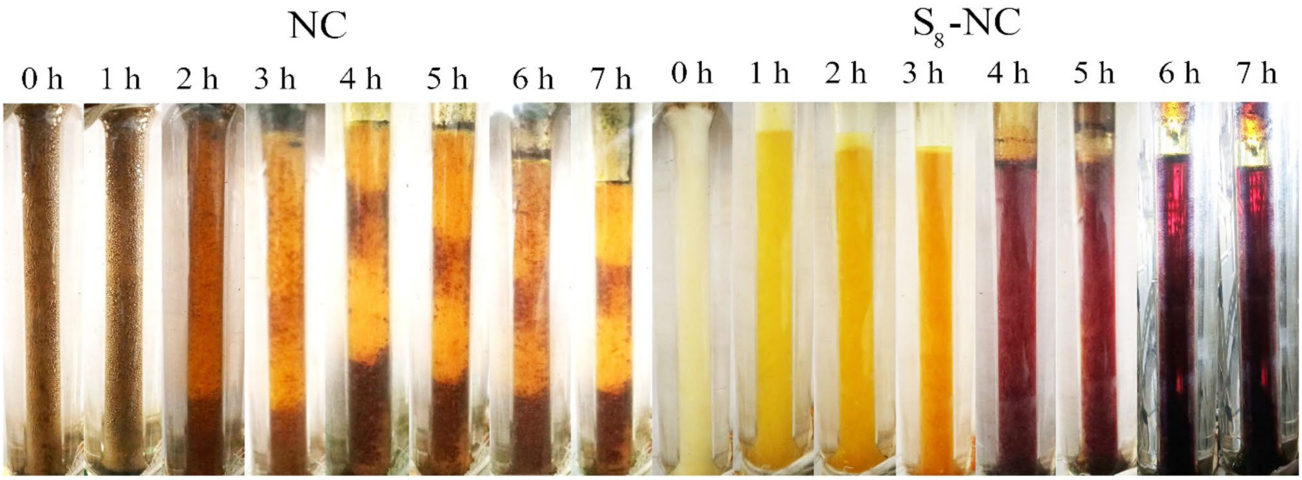

Fig. 3 Pictures of the bubble column reactor at different times during the reaction

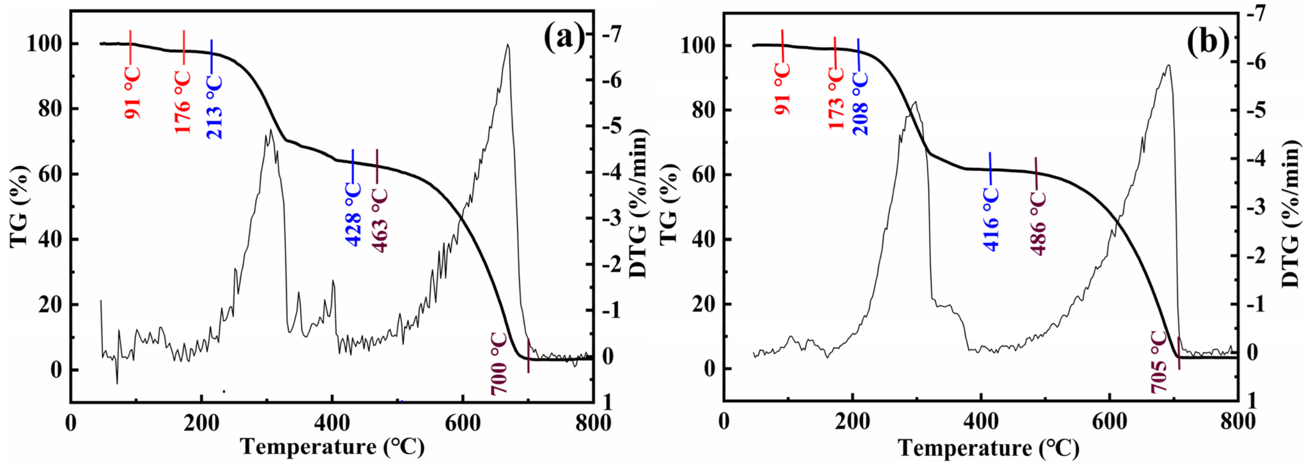

Fig. 4 TG/DTG thermograms **a** Fresh NC, **b** Fresh **S_8**-NC

Table 3 The crystals' weight loss rates of the fresh NC and **S_8**-NC catalysts

Catalysts	First stage (%)	Second stage (%)	Third stage (%)
Fresh NC	2.2	34.1	63.6
Fresh **S_8**-NC	1.0	37.5	61.5

performance and stability of **S_8**-NC compared to the control NC.

3.2.2 Catalysts Composition

Figure 4 shows the TG/DTG thermograms of the fresh NC and fresh **S_8**-NC catalysts. It is noticed that the weight loss of the catalytic system took place in the temperature ranges 90 °C–180 °C, 200 °C–430 °C and 460 °C–710 °C, and Table 3 shows the weight loss rates. The first stage of weight loss began at 90 °C for both catalysts, which was mainly due to the quality loss of crystal water [11, 12]. In the case of fresh NC, the second stage included the loss of NH_3 (relative molecular mass = 17), which was also confirmed by TPD-MS (Fig. S6). But for fresh **S_8**-NC, the second stage had a difference of 3.4%, due to the weight loss of the ligand, corresponding to the mass ratio of the **S_8**. The final stage of weight loss included the loss of CuCl.

3.2.3 Effect of the S_8 Additive on the Micromorphology of the Catalyst

In order to elucidate the crystal structure of Cu in the catalyst, we calcined fresh and used catalysts in a tube furnace under N_2 atmosphere at 450 °C for 0.5 h. Figure 5 shows the obtained XRD patterns of fresh and used catalysts. The diffraction peaks of CuCl were sharp and strong and no impurity peaks were found. Obviously, the diffraction peaks of the Cu (111) in used NC were less intense than in fresh NC. The diffraction peak of Cu (111) was weakened, probably due to the reduction or oxidation of Cu^+ [20, 21]. The addition of **S_8** did not change the diffraction peak of the Cu (111) after the reaction, indicating that **S_8** inhibited the loss of Cu. These results were also supported by the ICP analysis.

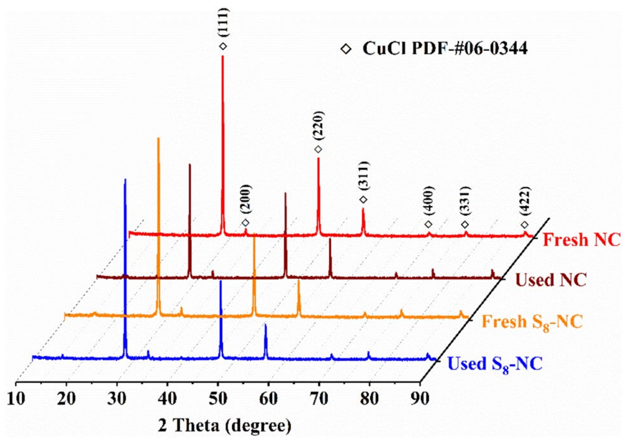

Fig. 5 XRD patterns of fresh and used catalysts

TEM and HRTEM images of fresh and used NC and fresh and used **S_8**-NC are shown in Fig. S7. Some irregular formations that can be observed in Fig. S7a are attributed to Cu crystals, while in the case of the fresh **S_8**-NC, several black spheres are detected in the TEM photo (Fig. S7c). Interestingly, it can be concluded that the active Cu component might exist in a spherical form in the fresh **S_8**-NC. As is shown in Fig. S7 e, f, g, and h, it can be found that the high crystallinity and the CuCl single-crystal. Typical d-spacing of 0.31 nm and 0.26 nm corresponded to the (111) and (200) planes of the CuCl crystal, respectively. Many CuCl (200) crystal faces (d = 0.26 nm) appear in fresh and used **S_8**-NC.

3.2.4 Effect of the Additives on the Catalysts' Functional Groups

Figure 6 shows the FT-IR spectra recorded to determine the functional groups of the fresh NC, **S_8**-NC catalysts and the pure **S_8** ligand. The strong bands at 3442.94 cm^{-1} and 1596.50 cm^{-1} of fresh NC corresponded to the vibration region of N–H bonds [11, 12, 22], which belong to NH_3. The strong bands at 3164.52 cm^{-1} corresponded to O–H groups, which correspond to chemisorbed water [23]. In case of the fresh **S_8**-NC, the vibration region of N–H bonds blue-shifted by approximately 0.59 cm^{-1} and increased in size compared to fresh NC, because the NH–NH_2 group (at 3431.63 cm^{-1}) of the ligand and Cu exists weak bonding action. Moreover, the strong band of the O–H groups blue-shifted by approximately 5.3 cm^{-1}, indicating that the O–H groups of **S_8** coordinate with Cu ions [24]. Therefore, it is concluded that the **S_8** is present in fresh **S_8**-NC and coordinates with Cu ions.

A portion of the modified catalysts were also characterized by FT-IR to further explore the effect of functional groups of ligands on the catalysts. Fig. S8a shows the FT-IR spectra of the fresh NC, **S_1**-NC, **S_5**-NC and **S_6**-NC, which illustrate the effect of amino-R-sulfonic (R = phenyl, none and naphthalene, respectively) for the catalysts. The obvious difference is that the peak of the N–H vibrational bond only appears in the FT-IR spectra of the fresh **S_1**-NC. It is inferred that the existence of benzene is beneficial to the catalyst. Fig. S8b shows the FT-IR spectra of the fresh NC, **S_1**-NC, **S_7**-NC and **S_8**-NC, indicate that effect of **N-**phenylsulfonic (N = amino, none and hydrazine, respectively) for the catalysts. No obvious peaks of N–H vibrational bond appear in the fresh **S_7**-NC. Meanwhile, the larger peaks of N–H vibrational bond in the fresh **S_8**-NC than other catalysts, which could be attributed to the existence of hydrazino group. Combined with the results of the catalytic activity, we can see that phenyl and hydrazino group play a vital role in highest catalytic activity of the **S_8**-NC among the modified catalysts.

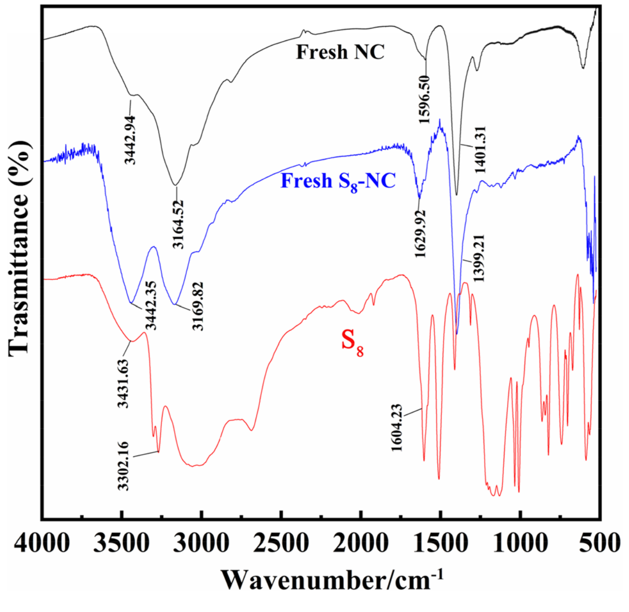

Fig. 6 FT-IR spectra of the fresh NC, fresh **S_8**-NC and the pure **S_8** ligand

3.2.5 Valence Changes of the Active Species

XPS analysis was carried out to investigate the chemical state and distribution of Cu species in the catalysts. Cu^+ is the main catalytic component in the acetylene dimerization and loss of this active component occurs in the reaction process with the formation of precipitate [25]. As shown in Fig. 7 and Table 4, peaks at 932.13 eV and 933.66 eV represented Cu^+ and Cu^{2+}, respectively [11, 12]. In the fresh **S_8**-NC, the peak position of Cu^+ was shifted (− 0.35 eV) due to the interaction between the ligand **S_8** and Cu^+, which leads to electron transfer from the ligand to the Cu^+ and increases the electron cloud density of Cu^+. This also demonstrated the coordination ability between the ligand and the active component (Cu). The content of Cu^{2+} in fresh **S_8**-NC was lower than that in fresh NC, while the Cu^{2+} content of the used NC and **S_8**-NC was 37.24% and 25.97%, respectively. Additionally, the metal ion content of Cu in the used NC and **S_8**-NC was 34.97% and 38.79%, respectively, while it is observed that the Cu loss in NC was twice than that of **S_8**-NC. These results, along with the pictures of the bubble column reactor (Fig. 3), prove that the addition of **S_8** inhibited the polymer formation, which in turn inhibited the loss of the active component (Cu^+).

4 Conclusions

The activity of the Nieuwland catalysts is generally hindered by deactivation that occurs during the reaction due to the high polymerization or oxidation of the active component, Cu^+. In this study, 4-hydrazinylbenzenesulfonic acid (**S_8**) was introduced as a stabilizer in the NC, and the **S_8**-NC catalytic system was studied in the context of the acetylene dimerization reaction. The catalytic system containing 5% **S_8** exhibited excellent catalytic performance and good stability. The yield of MVA was maintained at 42.9% at 80 °C, with an acetylene GHSV of 80 h^{-1}, which was increased by 18.8% over the control catalytic system. Moreover, the catalyst characterization proved that the addition of **S_8** increased the dissolution of CuCl in water, while it inhibited the

Fig. 7 **a** XPS spectra of the heating product of the catalysts for Cu 2p; **b** XPS spectra of Cu 2p 3/2 of the fresh and used catalysts

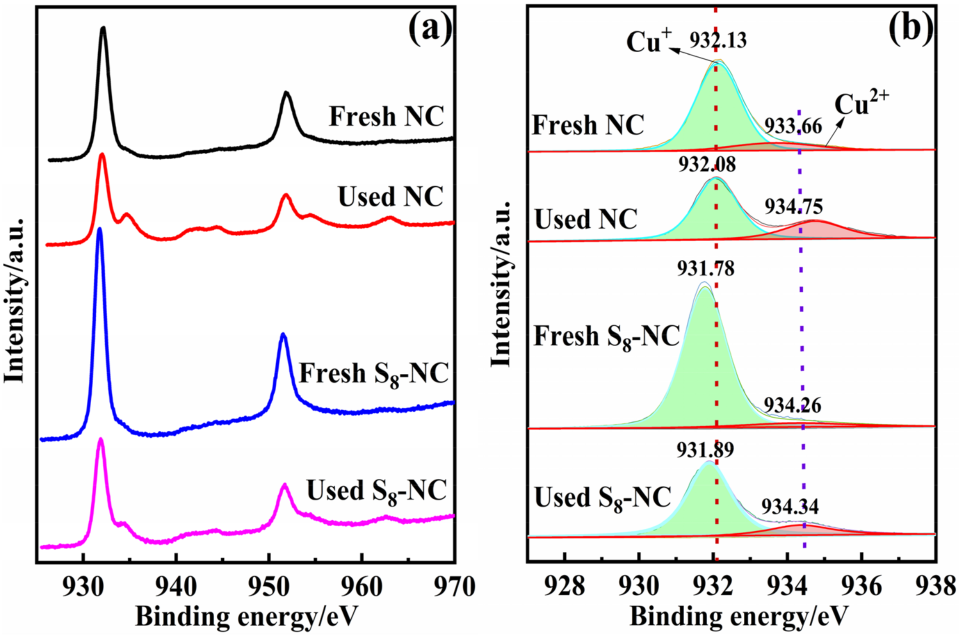

Table 4 The relative content and binding energy of Cu^+ and Cu^{2+} of the fresh and used catalysts, determined by XPS and ICP

Sample	Area% (Cu)[a]		Cu% (Metal ion content)[b]	Cu loss (%)
	Cu^+	Cu^{2+}		
Fresh NC	72.48	27.52	42.08	16.90
Used NC	62.76	37.24	34.97	
Fresh S_8-NC	76.89	23.11	41.98	7.60
Used S_8-NC	74.03	25.97	38.79	

[a] Determined by XPS

[b] Determined by ICP

polymer formation and the Cu loss that usually take place during the acetylene dimerization. Thereby, the addition of S_8 improves the activity and the long-term stability of NC catalysts, providing a powerful platform for further research of high-efficient catalysts.

Acknowledgements We acknowledge the National Natural Science Foundation of China (Nos. 21776179 and 21463021) for their financial support.

Compliance with Ethical Standards

Conflict of interest There are no conflict to declare.

References

1. Nieuwland JA, Calcott WS, Downing FB et al (1931) J Am Chem Soc 53:4197–4202
2. Nishiwaki K, Kobayashi M, Takeuchi T et al (2001) J Mol Catal A: Chem 175:73–81
3. White WC (2007) Chem Biol Interact 166:10–14
4. Ismail H, Leong H (2001) Polym Test 20:509–516
5. Carothers WH, Williams I, Collins AM et al (1931) J Am Chem Soc 53:4203–4225
6. Liu H, Xie J, Liu P et al (2016) Catalysts 6:120–131
7. Liu Z, Yu Y, Du J et al (2014) CIESC J 65:1260–1266 **(in Chinese)**
8. Lu J, Xie J, Liu H et al (2014) Asian J Chem 26:8211–8214
9. Lu J, Liu H, Xie J et al (2014) J Shihezi Univ (Nat Sci Ed) 32:213–217 **(in Chinese)**
10. Lu J, Liu H, Xie J et al (2015) Chem Eng 43:60–64 **(in Chinese)**
11. You Y, Luo J, Xie J et al (2017) Catalysts 7:394–404
12. You Y, Luo J, Xie J et al (2018) Catalysts 8:337–347
13. Chen R, Deng G, Mu R et al (1995) Chin J Inorg Chem 11:89–92 **(in Chinese)**
14. Amoozadeh A, Rahmani S (2015) J Mol Catal A: Chem 396:96–107
15. Otokesh S, Koukabi N, Kolvari E et al (2015) S Afr J Chem 68:15–20
16. Amoozadeh A, Golian S, Rahmani S (2015) RSC Adv 5:45974–45982
17. Amoozadeh A, Rahmani S, Bitaraf M et al (2016) New J Chem 40:770–780
18. Deng G, Mu R, Liu Z (1986) China Syn Rubber Ind 9:90–93 **(in Chinese)**
19. Liu J, Zuo Y, Han M et al (2012) J Nat Gas Chem 21:495–500
20. Zheng H, Ren J, Zhou Y et al (2011) J Fuel Chem Technol 39:282–286
21. Xiao Z, Wang X, Xiu J et al (2014) Catal Today 234:200–207
22. Poignant F, Saussey J, Lavalley J et al (1996) Catal Today 29:93–97
23. Biniak S, Pakuła M, Szymański G et al (1999) Langmuir 15:6117–6122
24. Ramli R, Khan MMR, Yunus RM et al (2014) Adv Nanoparticles 03:65–71
25. Tachiyama T, Yoshida M, Aoyagi T et al (2008) Chem Lett 37:38–39